In-depth influence of the top surface fabrication of a bead packing

Luc Oger and Renaud Delannay*
Univ. Rennes, CNRS, IPR [(Institut de Physique de Rennes)]-UMR 6251, F-35000 Rennes, France

Yves Le Gonidec
Univ. Rennes, CNRS, Géosciences Rennes-UMR 6118, F-35000 Rennes, France

(Received 2 December 2022; accepted 5 May 2023; published 26 May 2023)

Packings of beads confined in slowly tilted containers with a top free surface are commonly used in laboratory experiments to model natural grain avalanches and better understand and predict critical events from optical measurements of the surface activity. To that aim, after reproducible packing preparations, the present paper focuses on the effects of the surface fabrication, which can be scraped or soft leveled, on both the avalanche stability angle and the dynamic of precursory events for glass beads of 2-mm diameter. A depth effect of a scraping operation is highlighted by considering different packing heights and inclination speeds.

DOI: 10.1103/PhysRevE.107.054906

I. INTRODUCTION

Understanding the mechanics of granular flows is of first importance for numerous industrial and natural domains where avalanches constitute critical events of grain displacements. It remains difficult to prevent from such instabilities because the triggering is controlled by a large number of physical parameters, including the grain shape and material, the grain pile compacity and history and the ambient humidity and temperature. Aiming at identifying the contribution of each parameter, small-scale laboratory experiments are commonly performed in controlled conditions where the granular pile consists of grains confined in a box and slowly tilted until the granular flow at the top surface starts. At rest, a granular packing can sustain normal loads and shear stresses, such as a jammed structure [1]. When the packing is tilted, the shear stress may exceed a threshold, and part of the pile starts to flow and the macroscopic behavior of the packing is related to geometry changes of the contact network and more specifically to the nature of the contacts, which can be frictional, collisional, sliding, or cohesive [2]. Precursory events are observed during quasistatic behavior of the inclination process, i.e., when bead displacement occurs only when local shear forces reach a critical value defined by the Coulomb's friction law [3]. This behavior can be also influenced by the inclination speed of the grain container. For soft leveled surface flows, the critical shear stress is evidenced by the existence of the angle of maximum stability θ_A associated to internal friction properties [4]. When the tilt stops, the angle of the pile relaxes towards the angle of repose ($\theta_R < \theta_A$). Among the different techniques that can be used to observe the avalanche events of a granular pile, we can point out: measuring the weight at the outlet of the packing container [5], following the surface evolution by sequential optical [3,6,7] or acoustical [6,8,9] methods.

More recently, Kiesgen de Richter [10] and Kiesgen de Richter *et al.* [11] and Duranteau *et al.* [9] and Delannay *et al.* [12] have confirmed these observations by using two successive improved automatic tilting setups to study particular physical parameters that control the dynamic of grain avalanches. Indeed, the size of the system (height [5], length [6], width [13–16]), the density or volume compaction of the packing [5,6,17–19], and the tilting regime [12,20,21] are some parameters that have been studied in previous works. For example, Aguirre *et al.* [18] put in evidence the influence of the packing height h, which is related to an equivalent number n_l of bead layers in the container (see Eq. (1) in Ref. [18]) on the maximum stability angle when $n_l < 13$. This is particularly important when it consists in layer-by-layer depositions completed by a series of taps of the surface in between [3]. Indeed, this can be related to the well-known "wall effect" [22–26] obtained on few layers of grains that become quasiordered close to the walls of the container, which have locally modified the packing fraction.

Since many years, we have developed numerous experiments at the laboratory of the IPR (Institut de Physique de Rennes) to analyze precursory events of granular avalanches [9,10,12,27]. These previous series of experiments were the opportunity to identify ambient (proximity of a ventilation system, humidity, and temperature, etc.), experimental (dimensions and inclination speed of the container, physical parameters of the grains, synchronization of the data acquisition, etc.) and packing (electrostatic effects, compaction, fabrication, etc.) conditions that influence the reproducibility of the results. In particular, the fabrication of the granular packing (and its top surface), which is often considered in the literature as part of the "history" preparation of the grain packing, requires a particular attention for a better understanding of the results. First, the present paper focuses on the effects of the granular top surface fabrication on the dynamic of the packing destabilization. The parameters of the experimental setup, the fabrication of the grain packing with a top surface, which can be soft leveled or metal scraped, and the optical

*luc.oger@univ-rennes1.fr

experiments performed to detect the precursory events are described in Sec. II. Section III deals with the influence of the packing height on the precursors series of events and on the grain destabilization for a fixed inclination speed. In Sec. IV, the influence of the inclination speed is studied for some soft leveled or scraped top granular surfaces.

II. DESCRIPTION OF THE EXPERIMENTS

A. Experimental setup in controlled conditions

The grain packing is composed of glass beads pulled in a rigid container. As, by nature, critical events of the bead avalanches are very sensitive to all the ambient conditions of the laboratory, few experimental precautions were adopted. External mechanical vibrations exist in the laboratory so the whole experimental setup is, thus, mounted on an optical table (Melles Griot™) managed by four pneumatic attenuators and additional damping pads (Sunnex™ SP 700, 8-mm thickness) to isolate, as much as possible, the setup from the room floor submitted to low-frequency perturbations. To avoid the influence of the ambient humidity on the bead destabilization [28], the experiments are performed in an air-conditioned room where both the temperature (between 20–23 °C) and humidity (45–55% relative humidity (RH)) are controlled.

The bead container is a parallelepipedic metallic box (length $L = 440$ mm, width $W = 200$ mm and height $H = 200$ mm) and, to relax electrostatic effects inside the bead packing with a wire connection to the building ground. For our series of experiments, the available packing height h was selected between 30 and 185 mm. It is rigidly connected to a reclining plate, which rotates about two horizontal ball bearing axes positioned at the center of the length L to avoid possible inhomogeneous oscillations that may be due to weight momentum. The rotation is managed by the use of a linear actuator (SKF™): The maximum force of the working piston is 7 kN, and the stroke length is 700 mm. The speed is controlled, *via* an Arduino™ card by a main LABVIEW™ program written to control the whole experiment: the speed V_i ranges between 1.7 and 14°/min. The tilt angle is measured by the use of a Sensel™ sensor and recorded by the same program through an analogical/digital acquisition USB card: In our case, the angle θ ranges between the horizontal position and a maximum angle of 30° higher than the classical angle of maximal stability angle θ_A for simple sphere packings. The angle value is saved with the number of the image captured at the same time through a text file as described later on.

B. Fabrication of the bead packing

In addition to controlled environment conditions, reproducible experiments of bead destabilization also require a controlled protocol of the fabrication of the bead packing and, in particular, its granular top surface. Indeed, in the present paper, we achieved the so-called "same history" of a bead packing fabrication [29] aiming at performing reproducible experiments. The bead packing consists of monodisperse glass beads of diameter $D = 2$ mm (SiLiBeads type M™) randomly poured into the rigid bead container. The packing height $h < H$ is linked by an equivalent number n_l of bead layers in the container ($=2h/(\sqrt{3}D)$ [18]. For small n_l, the dynamic of the bead destabilization may depend on the bottom wall effect [22–26] defined previously. But this fact differs from precursors experiments from Aguirre *et al.* [5,18,30]. Indeed, in their experiments, a series of spoon taps on top of successive layer depositions have produced stronger and globally denser packings inside all the packing structures. This strong internal compaction induces, by consequence, two regimes for their avalanche mass versus the number of layers n_l (see Fig. 7 in Ref. [18]) and the appearance of their threshold close to 13. Below this threshold, a collective granular avalanche occurs due to short force chains interactions acting all along the packing; above this threshold, the successive deposition-compaction process induces internal rupture surfaces (between these depositions), which allow the appearance of a constant mass avalanche slipping at one rupture surface. This situation will not appear in our experiments as our fabrication conditions are strongly different as described now. During the preparation, a grid with a square mesh of 12 mm $\gg D$ is placed above the bottom of the bead container, then covered by the beads and then pulled out to homogenize and "dilute" the contact network between the beads in the whole packing volume. Then, the top free surface of the bead packing, i.e., the freely obtained surface, is finally flattened by horizontally pushing tool to remove surface irregularities larger than a bead diameter and form an average bead packing of height h.

In the present paper, series of experiments have been performed by the use of two different tools: a rigid metallic bar, commonly used in previous experiments [6,9,11], and a soft brush. Both tools have a width close to the inner box width. The first choice may compact and organize the superficial bead structure and result in a "scraped surface," and the second one only minimizes theses effects to maintain a "soft leveled surface." Our aim is to highlight the impact of these methods on the dynamic of the bead destabilization and on the precursors series of events.

According to this fabrication protocol, we have prepared series of bead packings with scraped or soft leveled surfaces and different heights h ranging between 30 mm ($n_l \approx 17$) and $H_{\max} = 185$ mm by inserting series of 5-mm thickness polyethylene foam plates at the bottom of the container.

C. Optical monitoring of the bead packing destabilization

To monitor the avalanche and precursory events of the bead packing during the inclination, an optical camera (Allied Vision™ Prosilica GC-2450) records images of the central part of the granular surface as a function of the tilt angle θ. The images, with a resolution of $S_0 = 2448 \times 2050$ pixels on eight bits gray level, are recorded with a rate of 1 image/s and a high shutter speed of 1/15 000 s to ensure image sharpness. This requires a proper lighting of the packing surface, provided by four LEDs stripes glued on both side of the camera support on a rigid metallic plate parallel to the beads packing surface, which turns coupled with the packing oscillation (see Fig. 1). The camera is fixed 1 m above the granular surface and the size of an image is the surface reference $S_0 = 230$-mm(length) $\times$ 200-mm (width). Note that a 2-mm diameter bead corresponds roughly to 25 pixels in an image.

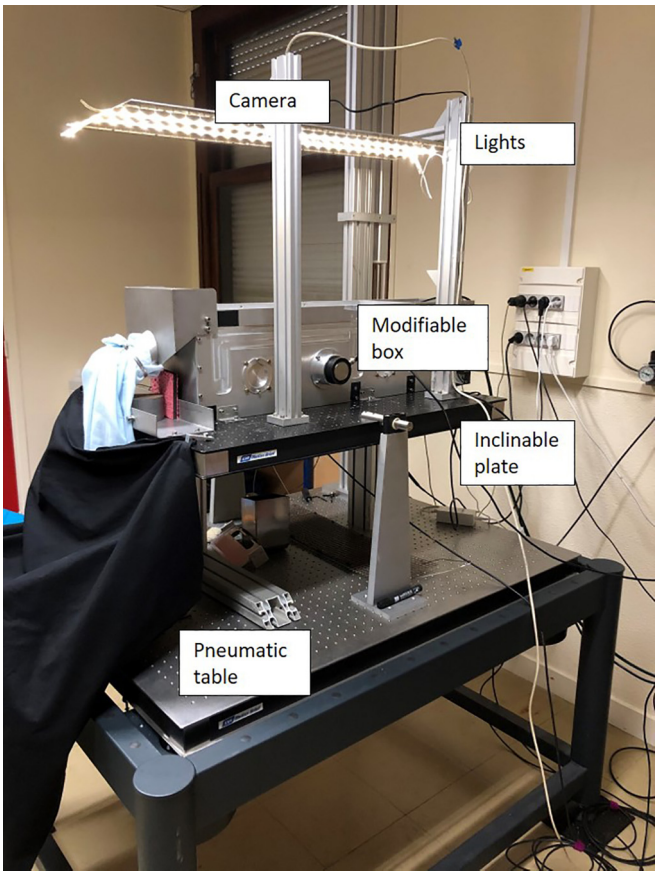

FIG. 1. Experimental setup which presents the pneumatic table, the inclinable plate, the metallic box, and the optical system (camera + lights) on top attached to the plate.

To detect and identify surface instabilities, we process the images according to previous approaches [6,9,28,31]: it is based on an Imagej [32] script, which consists in pixel differences of two consecutive images and an amplitude threshold to reduce the noise and quantify the amount of modified pixels S used to define the surface activity S/S_0 as a function of the angle θ (Fig. 2). We assume that a modified isolated small group of pixels is, by definition, linked to, at least, one bead surface displacement. Based on this ratio, the constant bead flow of the avalanche during a few seconds is associated with a nearly constant activity $S/S_0 \simeq 1$ measured for $\theta > \theta_A$ with θ_A as the avalanche angle (*maximum stability angle*).

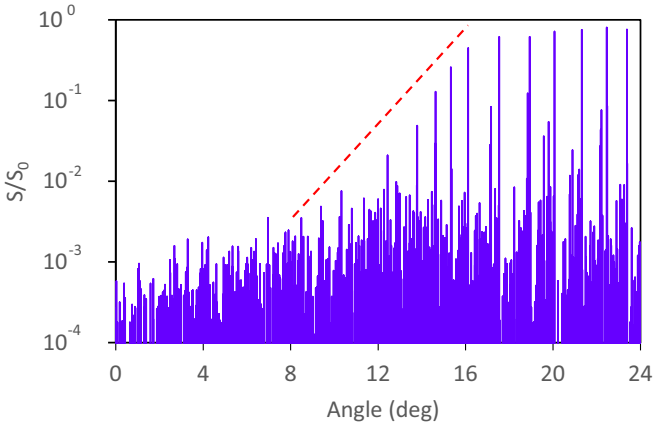

FIG. 2. Evolution of S/S_0 versus the tilting angle θ. The dashed line is a possible technique to extend the basic threshold approach for small precursor observation.

In Fig. 2, we can extract the first precursor θ_p (*first appearance angle*) and θ_A for each individual experiment, N_p precursory events can be identified, characterized by peaks of activity located at quasiregular tilt angles $\Delta\theta$ according to

$$\theta_A \approx \theta_p + N_p \Delta\theta, \tag{1}$$

by assuming that $\Delta\theta$ is the mean value of the interprecursor angles measured during each experiment. This quasiregularity of the interprecursor $\Delta\theta$ was first noed by Nerone *et al.* [3]. This fact is still not yet perfectly understood. According to the experimental fluctuations observed on θ_p, N_p, and $\Delta\theta$, during each experiment, the rough extension of this equation used in the following figures for their mean values is only presented to provide some hints. In the following, these parameters are used to quantify the dynamic of the bead packing activity during gravity destabilization.

But, at lower tilt angles, the extraction of a clear first precursor θ_p from the signal noise is not so obvious (see Fig. 2) and can be assessed, at a first approach, as the first angle associated with $S/S_0 > 0.5$. The choice of the threshold equal to 0.5 is arbitrary but not crucial for the observation of the precursors series of events versus height and speed. According to Eq. (1), diminishing this threshold will just add few "previous" precursors for all the studied cases here. At this threshold, small error bars for the interprecursor values are observed, and an automatic treatment process can be used. In another way, if we try to adjust this threshold by fitting down the series of first precursors according to the slope drawn in Fig. 2 (dashed line), it is unclear to define the correct value versus the minimal signal to noise ratio. For example here, which value can be selected $S/S_0 = 2\%$ at $\theta_p = 12^\circ$ or $S/S_0 = 0.35\%$ at $\theta_p = 8.4^\circ$? The first choice is "compatible" with a visible precursor measurement, which is not true for the second choice where S/S_0 is smaller than the noise measurement made later on around 12°. This problem will imply individual and manual treatment for each experiment and will increase the error bars.

III. DYNAMIC OF A SOFT LEVELED OR SCRAPED BEAD PACKING

By performing a series of experiments for different heights h of the bead packing and a fixed inclination speed of 3.3°/ min, we study the influence of the method for leveling the top granular surface with a soft (named here soft) or rigid tool (named here scraped").

A. Behavior of the maximum stability angle

A series of bead packings have been prepared in a container according to the method described in Sec. II B. An experiment consists of a slowly tilting of the bead container up to the avalanche, which occurs at the maximum stability angle θ_A (Fig. 3). A set of a minimal number of 10 up to 20 identical experiments have been performed in order to obtain a good

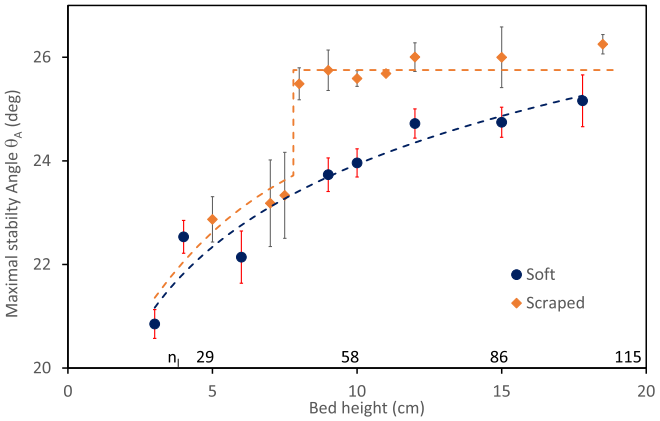

FIG. 3. Maximum stability angle θ_A measured as a function of the packing height for soft (disks) or scraped (diamonds) leveling top surfaces. Error bars are associated to, at least, ten similar experiments.

mean value for a set of given conditions. Indeed, note that experiments performed in the same conditions have classically $10-15\%$ of natural fluctuations induced by different bead organizations of the packings [33]. This is the main reason of the production of a large number of successive independent experiments to obtain a correct mean value for our measurement.

Soft leveling surface experiments are characterized by a continuous increase in the maximum stability angle θ_A with the packing height h (Fig. 3, disks). By construction, the full packing structure is only controlled by the initial extraction of the bottom grid, which creates a dilute stable homogeneous packing. So, this evolution is only linked to the classical effect of the hydrostatic pressure of successive layers and of h, the distance between the bottom wall and the top surface, which defines also the decreasing influence of the classical bottom wall effect mentioned previously. Interestingly, the nonlinear regression curve can be also interpreted as the increase in the probability of the grains inside the packing to present more local contacts, which can slip linked to more and more complex force chain structures [34].

For the scraped surface experiments, angle θ_A presents two distinctive behaviors depending on h compared to a critical height $h_c = 7.8$ cm. When $h < h_c$, angle θ_A follows a similar increase as the soft case with the packing height h, which is visible by an identical dashed fit line on Fig. 3. When $h > h_c$, angle θ_A remains constant with the packing height h. Before going deeper in the analysis of these different behaviors and according to the observations made by Aguirre *et al.* [5]. which linked the avalanche angle to the packing density, we will look at the different packing fractions obtained by these different preparation techniques.

To quantify this influence, we have measured global packing fractions for several piling heights below (5 cm) and above (10 cm) the transition limit, and at the maximum height (18.5 cm) for both soft leveled and scraped surfaces. Each individual packing fraction measurement was obtained by following exactly the same fabrication process described in Sec. II B for the packing preparation. Then, we fully empty the container and weight the amount of grains present on it.

TABLE I. Packing fraction versus height and surface layering techniques.

Height (cm)	Scraped	Soft
5	0.635 ± 0.002	0.555 ± 0.005
10	0.608 ± 0.001	0.579 ± 0.001
18.5	0.603 ± 0.001	0.591 ± 0.001

The results are averaged on five-independent measurements to estimate the mean and standard deviations for each configuration (Table I).

By looking at the packing fractions for the different heights, we can confirm the small influence of the soft leveling technique on the packing fraction visible by just a small continuous increase in the packing fraction with h, which can be linked to the ρgh effect. The packing fraction for $h = 5$ cm is close to the random loose packing (RLP) (typically about 0.55), which confirms the dilution process generated by the moving grid during the packing fabrication.

By opposition, during the scrapping action, we can observe a "rolling moving" bump of beads in front of the rigid tool all along the top surface displacement, which densifies a lot the packing superficially. Indeed, this effect is clearly visible when $h = 5$ cm: the packing fraction is very close to the random close packing (RCP) (typically about 0.64), which is high for classical piling experimental setups. When the packing heights are larger, the influence of the densest upper thickness diminishes as visible for the two other values of h (10 and 18.5 cm) which are "identical" and close to 0.60. The strong difference of the packing fractions for the two packing preparations for $h = 5$ cm and the identical behaviors for the θ_A evolutions imply that the correlation between packing fractions and avalanche angles made by Aguirre *et al.* [5] cannot be applied in our cases. These similar behaviors for θ_A at small heights implies that the avalanche events are mainly controlled by the destabilization (such as Weibull's rupture) of the force chains that cross the packing independently of the local packing fraction. Indeed, for small packing heights, these force chains cross all the packing and cannot be supported by the smooth bottom walls. So they can be more easily broken through all these packing thickness.

As already mentioned, for larger heights, this densification action is, of course, space limited to a "small" thickness under the top surface only managed by the surface preparation. This structure discontinuity can explain the constant angle of avalanche for the scraped case due to the avalanche rupture which appears just below this constant denser thickness zone.

In complement, we can note that, close to very large heights available (value of 18.5 cm in the present paper), the maximum stability angles θ_A tend to be similar for the soft leveled and the scraped surface experiments around $25^\circ \pm 0.5$, which confirms the decrease in the influence of the denser upper packing thickness.

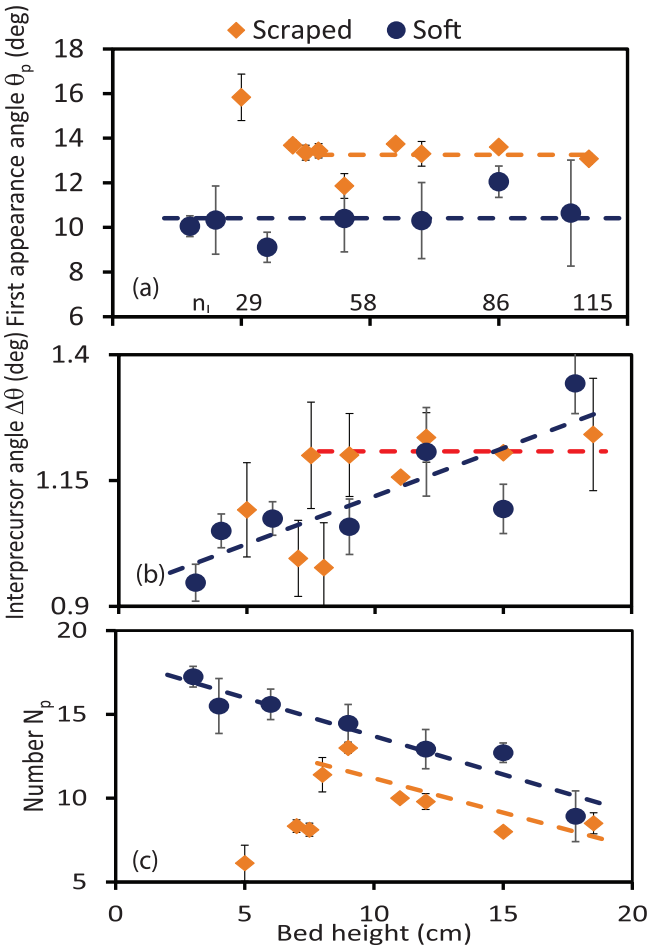

FIG. 4. Characteristic parameters of the precursory events measured as a function of the packing height with soft leveled (disks) or scraped (diamonds) surfaces. (a) θ_p, the first precursor angle; (b) the interprecursor angle $\Delta\theta$ and (c) the number N_p of precursors events.

B. Behavior of the precursory events

Before the avalanche occurs at the maximum stability angle θ_A discussed above, N_p precursory events can be detected during each experiment [Fig. 4(c)]: The first event occurs at the angle θ_p [Fig. 4(a)] and the angle step between successive events is $\Delta\theta$ [Fig. 4(b)].

For soft leveled surface experiments, the first appearance angles range between 9.6 and 11.3 ° with large uncertainties up to 40% because these events are associated with large local packing fluctuations, which induce weak surface activities defined by an arbitrary threshold of $S/S_0 = 0.5$ (see Sec. II C). The dependency between θ_p and h is, thus, not obvious, which implies that, for simplicity, we have drawn the same slope as the scraped case described below. The interprecursor angle $\Delta\theta$, defined as an average parameter over N_p observations, is more representative of the dynamic of the bead destabilization: It ranges between 0.9 and 1.4 ° and as a first approximation, it linearly increases with the packing height. From Eq. (1), the number N_p of detected events decreases also with h.

For scraped surface experiments, when $h < h_c$, θ_p, $\Delta\theta$, and N_p are hardly measurable. This behavior can be related to the measurements of $h = 5$ cm in Table I, which show a dense RCP jamming structure avoiding small internal displacements (slips) before large tilting angles and, by consequence, close to the final avalanche angle θ_A. This explains why N_p is very small and the uncertainties for θ_p and $\Delta\theta$ are large in this part of h. When $h > h_c$, measurements of $\theta_p \approx 13.5$ ° and $\Delta\theta \approx 1.2$ °, are drawn as constant and more reproducible than for soft leveled surfaces: scraping the surface tends to compact the superficial bead layer for which effects are an increase in the stability angle and stronger events associated with larger activities, i.e., events for $S/S_0 > 0.5$ can be detected with more confidence. In complement, we have drawn the same linear slope (as an eye guide) for the evolution of N_p as for the soft case: only the initial values are different. According to Eq. (1), in the first approximation, it is not true but a constant evolution seems not so valid. Both decreases in N_p in our range of h is quite interrogating about their evolutions for higher h: N_p is going down to 0 or converging to a minimal value? We have not yet the answer due to the limitation of our setup.

IV. INFLUENCE OF THE INCLINATION SPEED

Up to now, we have assumed that the tilting process is a quasistatic process, but we know that it is not perfectly true, so we study how the inclination speed biases our experimental results. In this section, we study the influence of the packing inclination speed, in the range of 1.7–14°/min on the avalanche and precursory events. For each experimental speed conditions, we have also reproduced between 8 and 15 similar experiments to highlight representative results. The choices of the different heights and surface association analysis was induced by the observation of θ_A in Fig. 3: We selected for the first soft leveled surface experiments $h = 4$ cm $\ll h_c$, then, for both soft and scraped ones 10 cm $> \approx h_c$ and, finally, for scraped surface experiments $h = 18.5$ cm $\gg h_c$.

A. Behavior of the maximum stability angle

As previously, for each experiment, we measure the maximum stability angle θ_A of the bead packing. The results are plotted in Fig. 5, which also shows the error bars of the measurements for both soft leveled and scraped surfaces.

Soft leveled surface experiments are characterized by a continuous nonlinear increase in the maximum stability angle θ_A with the inclination speed: It increases from 22.2 to 23.5° for a packing height of $h = 4$ cm, and the behavior is similar for $h = 10$ cm where θ_A increases from 23.4 to 24.5°. The small increase is linked to the increase of the amount of beads, which implies higher internal stability. Indeed, the effect of h observed here is in agreement with the previous analyzes dedicated to the effects induced by the packing height (Fig. 3). In these soft leveled cases, the contact stiffness is weak, and the superficial beads are more sensitive to inertia effects, which increases with the inclination speed, in agreement with previous experiments [35–37].

For the scraped surface experiments as we are at a height $h > h_c$, we can observe also here a nearly constant maximum stability angles θ_A, about 25.7 and 26.5° for packing heights $h = 10$ and 18.5 cm, respectively. The difference of 0.8° can

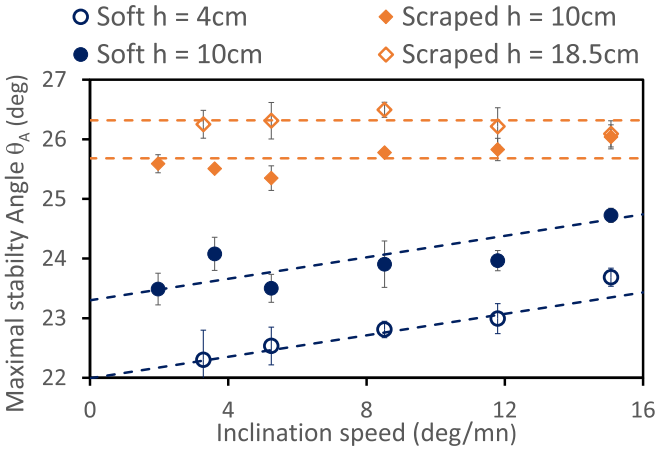

FIG. 5. Maximal stability angle θ_A measured as a function of the inclination speed with soft leveled (disks) or scraped (diamonds) surfaces and different packing heights. The dashed lines for the scraped surfaces are drawn horizontally and, for the soft leveled surface, they are just drawn for eye guides without theoretical explanations. Error bars are associated with 8–15 similar experiments.

fall into the uncertainty of the measurements performed for the previous analyzes (Fig. 3), already pointed out and justified the horizontal line on the Fig. 3 for $h > h_c$.

B. Behavior of the precursory events

We also measured the characteristic parameters θ_p, $\Delta\theta$, and N_p associated with the precursory events, and we plotted their evolutions in Fig. 6.

When the inclination speed increases, the uncertainties of the first precursor appearance increase naturally due to two additional effects coupled with the inertial effect: temporal angular resolution (still only one image per second) and higher inherent vibrations of the full setup linear actuator.

In Fig. 6(a), we can also note that, only for the soft leveled surface (empty circle) at $h = 4$ cm, the first precursor appearance angle θ_p increases with the inclination speed: The value starts around $\sim 10.5^\circ$ ends around $\sim 16^\circ$. For the other three cases, the scraped surface $h = 10$ cm (full diamond) and 18.5 cm (empty diamond) and the soft case $h = 10$ cm (full circle), the first precursor appearance angles θ_p remain constant in the full range of the inclination speed. For the scraped cases, this observation is in accordance with the previous observation of the nondependence of the maximal stability angle θ_A, which indicates that the denser superficial thickness zone limits the displacement of the beads. On the other hand, for the soft case at $h = 10$ cm the observation of a constant value of θ_p with the inclination speed is more complex to explain: we may assume that the dense packing fraction (see Table I) allows the existence of long force chains crossing all the height of the piling and keeping some stress independently of the inclination speed.

Figures 6(b) and 6(c) show the coupled information about $\Delta\theta$ and N_p versus the inclination speed. As previously noted, we can observe globally that for the scraped surface, these two parameters are constant, and for the soft leveled surface, they

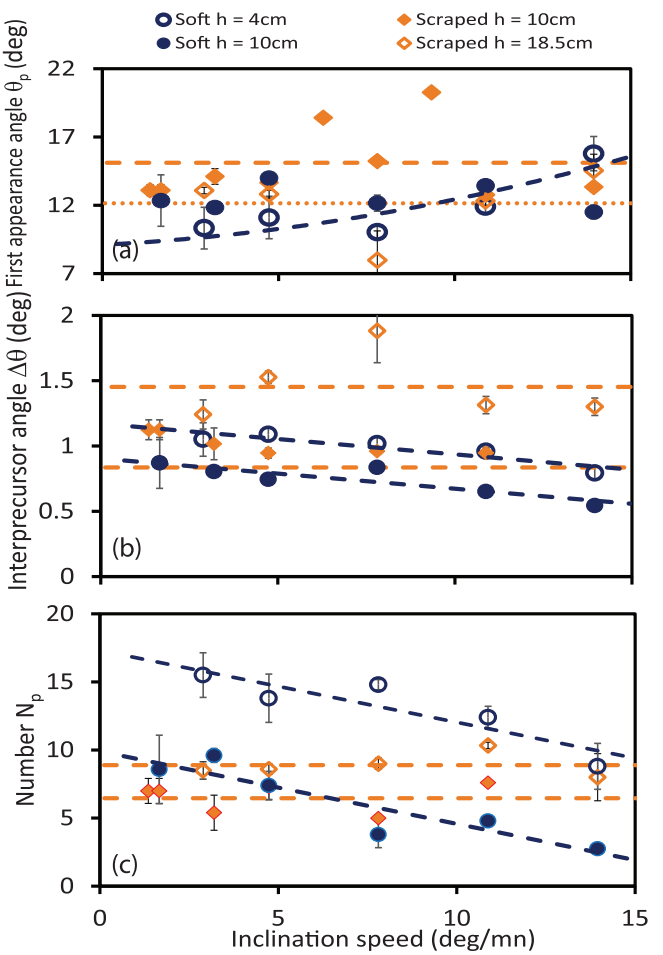

FIG. 6. Characteristic parameters of the precursory events measured as a function of the inclination speed with soft leveled (disks) or scraped (diamonds) surfaces and different packing heights. (a) represents the average of first precursor appearance angle θ_p. (b) and (c) are coupled to represent the behavior between $\Delta\theta(i)$ and $N_p(i)$. The unique dotted line represents simultaneously the soft case for $h = 10$ cm and the scraped case for $h = 18.5$ cm. The dashed lines represent the two other cases (soft for $h = 4$ cm and scraped for $h = 10$ cm).

vary due to less and less internal superficial stress for smaller height h or higher speed.

Indeed, with a soft leveled surface, the packing is characterized by both an interprecursor angle and a number of interprecursors that decrease linearly with the inclination speed. The interprecursor angles $\Delta\theta$ vary roughly from 1° to 0.7° for $h = 4$ cm and from 0.9 to 0.6° for $h = 10$ cm. The numbers of interprecursors N_p vary at the same time from 15 to 10 for $h = 4$ cm and from 10 to 0 for $h = 10$ cm. We have to mention that for the inclination angle higher than 18°, some small superficial continuous slidings of top grains can appear without producing an avalanche, which make the optical detection of precursors impossible in these cases. Of course, this problem avoids the use of these data for the averaging.

With a scraped surface, the packing is characterized by a constant interprecursor angle $\Delta\theta$ about 1.5° for $h = 18.5$ cm and about 1° for $h = 10$ cm. N_p is about nine precursors for

$h = 18.5$ cm and about seven for $h = 10$ cm. These results confirm also the observation made previously for the other scraped surface results: no evolution of parameters with either the height or the inclination speed for values of height higher than the transition limit of h_c (see Sec. III A). Indeed, the upper dense thickness generated by the scrapping process controls strongly the appearance of the precursor events by "blocking" the displacements of the beads inside this thickness.

V. DISCUSSION AND CONCLUSION

The analysis of around 8 to 20 identical experiments (i.e., same history of fabrication and physical and mechanical parameters) have allowed us to use them with enough good reproducible results to deduce some conclusions about these different experimental protocols.

In the classical results [3,5–7,18] the maximal stability angle θ_A and the precursor appearances were observed only on packings submitted either to series of tapping or to superficial scrapping techniques. But here, we have demonstrated that the packing preparation history (i.e., soft leveled or scraped surface) is crucial in these kinds of studies and can explain some particular previous results. In our cases, we have observed that the soft leveled surface cases are, always, producing more evolving results than the scraped ones. These behaviors are due to the more dilute, homogeneous packing structure for the soft cases by opposition of the presence of a dense reorganized thick upper band in the scraped cases. We have pointed out that the decreases of N_p in our range of h is generating new interrogations about either the full disappearance of the precursors or a small remaining number of them. This needs setup development and complementary investigation. Another interesting point for a practical use is the fact that scraping the surfaces implies that the experiments can be performed at a "higher inclination" speed, allowing performing a larger number of experiments when our studies require large statistical approaches and less uncertainty results.

Main results and conclusions are defining the good use for our future works made in our laboratory for studying more complex behaviors, such as playing with different lengths and widths of the box, inclination speed, oscillation cycles $\pm\theta_c$, environmental conditions RH or adding other detection techniques, such as mechanical or acoustical sensors.

ACKNOWLEDGMENTS

We thank P. Chasle for all the developments of our LABVIEW^{TM} code and Y. Robert and G. Pecheul for the mechanical realizations.

[1] A. J. Liu and S. R. Nagel, Annu. Rev. Condens. Matter Phys. **1**, 347 (2010).
[2] L. Oger, A. Vidales, R. Uñac, and I. Ippolito, Granular Matter **15**, 629 (2013).
[3] N. Nerone, M. A. Aguirre, A. Calvo, D. Bideau, and I. Ippolito, Phys. Rev. E **67**, 011302 (2003).
[4] Y. Zhang and C. S. Campbell, J. Fluid Mech. **237**, 541 (1992).
[5] M. A. Aguirre, N. Nerone, I. Ippolito, A. Calvo, and D. Bideau, Granular Matter **3**, 75 (2001).
[6] S. Kiesgen de Richter, G. Le Caër, and R. Delannay, J. Stat. Mech.: Theory Exp. (2012) P04013.
[7] M. Duranteau, Dynamique granulaire à l'approche de l'état critique, Ph.D. thesis, Université Rennes 1, 2013.
[8] V. Y. Zaitsev, P. Richard, R. Delannay, V. Tournat, and V. E. Gusev, Europhys. Lett. **83**, 64003 (2008).
[9] M. Duranteau, V. Tournat, V. Zaitsev, R. Delannay, and P. Richard, in *Powders and Grains 2013*, Vol. 1542 (AIP, Melville, NY, 2013), pp. 650–653.
[10] S. Kiesgen de Richter, Etude de l′organisation des réarrangements d′un milieu granulaire sous sollicitations mécaniques, Ph.D. thesis, Université de Rennes1, 2009.
[11] S. Kiesgen de Richter, V. Y. Zaitsev, P. Richard, R. Delannay, G. Le Caër, and V. Tournat, J. Stat. Mech.: Theory Exp. (2010) P11023.
[12] R. Delannay, M. Duranteau, and V. Tournat, C. R. Phys. **16**, 45 (2015).
[13] P. Boltenhagen, Eur. Phys. J. B **12**, 75 (1999).
[14] S. Courrech du Pont, P. Gondret, B. Perrin, and M. Rabaud, Europhys. Lett. **61**, 492 (2003).
[15] W. Bi, R. Delannay, P. Richard, N. Taberlet, and A. Valance, J. Phys.: Condens. Matter **17**, S2457 (2005).
[16] J. Métayer, Stabilité et propriétés rhéologiques d'empilements granulaires confinés., Ph.D. thesis, Université de Rennes I, 2008.
[17] P. Evesque, D. Fargeix, P. Habib, M. P. Luong, and P. Porion, J. Phys. I **2**, 1271 (1992).
[18] M. A. Aguirre, N. Nerone, A. Calvo, I. Ippolito, and D. Bideau, Phys. Rev. E **62**, 738 (2000).
[19] N. Gravish and D. I. Goldman, Phys. Rev. E **90**, 032202 (2014).
[20] A. Kabla, G. Debrégeas, J.-M. di Meglio, and T. J. Senden, Europhys. Lett. **71**, 932 (2005).
[21] A. Jarray, V. Magnanimo, and S. Luding, Powder Technol. **341**, 126 (2019).
[22] D. Mehta and M. C. Hawley, Ind. Eng. Chem. Process. Dis. Dev. **8**, 280 (1969).
[23] L. Oger, J. P. Troadec, D. Bideau, J. A. Dodds, and M. J. Powell, Powder Technol. **46**, 121 (1986).
[24] Y. Bertho, F. Giorgiutti-Dauphiné, and J.-P. Hulin, Phys. Rev. Lett. **90**, 144301 (2003).
[25] W. Dai, J. Reimann, D. Hanaor, C. Ferrero, and Y. Gan, Granular Matter **21**, 26 (2019).
[26] J. Lin, H. Chen, R. Zhang, and L. Liu, Mater. Charact. **154**, 335 (2019).
[27] L. Oger, R. Delannay, and Y. Le Gonidec, EPJ Web Conf. **249**, 03023 (2021).
[28] L. Oger, C. el Tannoury, R. Delannay, Y. Le Gonidec, I. Ippolito, Y. L. Roht, and I. Gómez-Arriaran, Phys. Rev. E **101**, 022902 (2020).

[29] D. Bideau, E. Guyon, and L. Oger, in *Disorder and Fracture*, NATO ASI Series Vol. 204, edited by J. C. Charmet, S. Roux, and E. Guyon (Springer, Boston, MA, 1990), pp. 255–268.
[30] M. A. Aguirre, N. Nerone, A. Calvo, I. Ippolito, and D. Bideau, *Traffic and Granular Flow* (Springer, Berlin/New York, 2000), pp. 489–494.
[31] N. Nerone, M. Aguirre, A. Calvo, I. Ippolito, and D. Bideau, Physica A **283**, 218 (2000).
[32] C. Schneider, W. Rasband, and K. Eliceiri, Nat. Methods **9**, 671 (2012).
[33] E. Guyon and J. P. Troadec, *Du sac de billes au tas de sable* (Odile Jacob, Paris, France, 1994).
[34] S. J. Antony, Philos. Trans. R. Soc. A **365**, 2879 (2007).
[35] G. H. Ristow, Europhys. Lett. **34**, 263 (1996).
[36] A. Jarray, V. Magnanimo, M. Ramaioli, and S. Luding, Powders and Grains, EPJ Web Conf. **140**, 03078 (2017).
[37] T. Pöschel and V. Buchholtz, Chaos, Solitons Fractals **5**, 1901 (1995).